*Revised Manuscript with No Changes Marked

Power to Gas-Biomass oxycombustion hybrid system: Energy integration and potential applications

Manuel BAILERA[a], Pilar LISBONA[b], Luis M. ROMEO[a], Sergio ESPATOLERO[a]

[a] Research Centre for Energy Resources and Consumption (CIRCE) - Universidad de Zaragoza, CIRCE Building – Campus Río Ebro, Mariano Esquillor Gómez, 15, 50018 Zaragoza, Spain

[b] Escuela Universitaria de Ingenierías Agrarias de Soria - Universidad de Valladolid, Campus Universitario Duques de Soria, 42004, Soria, Spain.

Abstract

A promising hybridization which increases the chances of deployment of power to gas technology is found in the synergy with oxycombustion of biomass. This study assesses the efficiency of an energy integrated system under different sizes and potential applications. District heating and industrial processes are revealed as the most suitable potential applications for this hybrid technology. Global efficiency of the combined system may be increased through thermal energy integration. The relative increment of efficiency achieved for those designs which avoid the requirement of an air separation unit and for those which completely consumed the generated CO_2, are 24.5% and 29.7% respectively. A 2 MWth district heating case study is also analysed, revealing that 81.2% of the total available heat from the PtG-oxy system could be integrated raising the global efficiency up to 78.7% at the adequate operational point. Further 'full-fuel-cycle' analysis will be required prior to decide the interest of the concept under a specific scenario in comparison to other available energy storage technologies.

Keywords

Power-to-Gas, Oxycombustion, Methanation, Oxyfuel, Integration

Corresponding author: pilar.lisbona@unizar.es, Tel: +34 876 552 196, Fax: +34 976732078

1. Introduction

In the mid-term, one of the most promising energy storage technologies might be the Power to Gas (PtG) process [1]. Strictly, renewable electricity is converted to fuel gas by means of electrolysis, storing electrical energy in form of hydrogen. Then, the generated H_2 can be combined with carbon dioxide to produce methane through the Sabatier reaction [2].

$$CO_2 + 4H_2 \leftrightarrow CH_4 + 2H_2O \qquad \Delta H_{298K} = -165\ \mathrm{kJ/mol} \qquad \text{(Eq. 1)}$$

The availability of a suitable source of CO_2 is the main limiting factor when assessing the potential of Power to Gas deployment in a region; reducing considerably the geographic location possibilities for this technology [3]. Therefore, the access to a continued carbon dioxide flow to be fed to the PtG process becomes a crucial issue that must be properly addressed.

Biogas plants, waste managers, industries and power plants are the largest CO_2 sources and the most interesting partners for integration with PtG [4]. Nevertheless, attention must be focused on the last two options since their efficiencies will be strongly penalized when the operation of carbon separation technology is accounted.

Biogas is mainly composed by methane (50 – 85 %) and carbon dioxide (15 – 50 %) [5], so a direct conversion of CO_2 without previous separation is possible, avoiding the energy penalty associated to carbon capture. Due to this advantage, some of the major PtG projects in the world perform directly the methanation of the biogas (MeGa-store 4.7 MW [6], Erdgas Schwaben 1.0 MW [7], and P2G-BioCat 1.0 MW [8]). Similarly, waste management plants produce a gas mixture of CH_4 and CO_2, but it is usually burnt for self-consumption given its low quality [9].

Power plants and most industries generate CO_2 during fuel combustion for electric or thermal energy production. However, carbon dioxide concentration in flue gas is low and capture costs up to 75 €/t_{CO2} depending on CO_2 concentration [10]. Therefore, the hybridization of PtG-Oxycombustion is proposed as a method that avoids the capture penalty and allows the direct comparison between biogas upgrading and flue gas methanation.

51 During oxycombustion, a mixture of recycled flue gas and pure oxygen is used as comburent
52 instead of air [11]. Thus, the large N_2 content is substituted by the combustion products (mainly
53 CO_2 and H_2O), and flue gas can achieve a high carbon dioxide concentration once steam is
54 condensed. Energy penalty associated to this capture process comes from the air separation unit
55 (ASU) that produces pure oxygen from air with a 190 kWh/t_{O2} average consumption [12].
56 However, with an adequate size design of the PtG-Oxycombustion system, the by-produced
57 oxygen from electrolysis can replace the requirement of the ASU.
58 Furthermore, biomass has been selected as fuel for oxycombustion boiler to convert the process
59 into an entirely carbon neutral one. As the carbon dioxide used in the methanation process
60 comes from biomass combustion, the generated synthetic natural gas (SNG) will be equally
61 carbon neutral.
62 The scope of this study is to analyse the possible applications of hybrid PtG-Oxycombustion
63 systems depending of its size and operation conditions. Methanation process and CO_2
64 compression produce extra thermal energy that can be useful. The maximum potential
65 increment of the efficiency associated to complete integration of these heat streams is also
66 calculated.
67 Since the target of the work is to clarify what applications are feasible depending on the most
68 suitable operation point for every size scale, the integrated system is characterized without
69 regarding any external loss that will penalize the profit of the concept. Prior to decide the
70 interest of the concept under a specific scenario in comparison to other available energy storage
71 technologies, further 'full-fuel-cycle' analysis should be performed.

72 **2. Hybrid system description**

73 The proposed configuration is a hybrid system which combines an oxyfuel boiler and a Power
74 to Gas plant. A source of renewable energy supplies power to the electrolysers in the system
75 (Figure 1) to store a constant amount of electricity in the form of hydrogen also co-producing
76 oxygen. The oxygen generated in the electrolysers might be used to partially or completely

cover the comburent demand in an oxyfuel boiler. In this way, the efficiency of this process is increased since the power consumption of the ASU would be reduced or even avoided. Additionally, methanation takes place between the CO_2 contained in the flue gas from the oxyfuel thermal plant and the hydrogen from electrolysis to produce synthetic natural gas. If the flue gas is not completely consumed in methanation, the remaining can be directed to the compression train for transportation and storage.

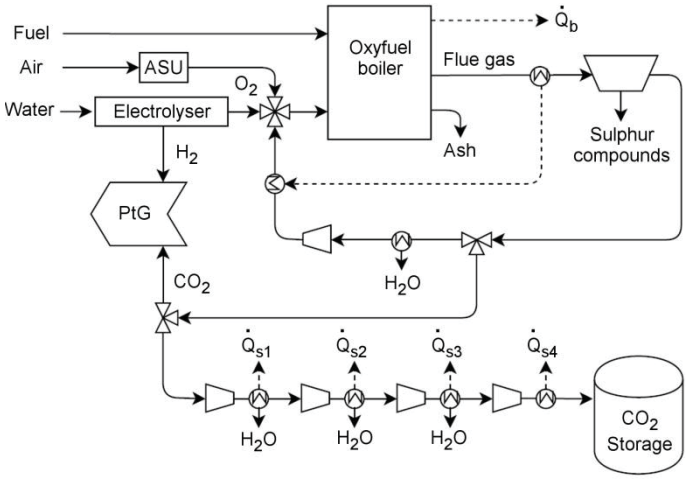

Figure 1. Block diagram of the hybrid power system.

In a prior study, the different operation ranges of the installation were obtained through simulation for a coal-fired oxyfuel boiler [13]. The analysis was performed by means of the definition of ξ_{oxy}, the ratio between the energy contained in hydrogen produced by electrolysis ($LHV_{H2} \cdot \dot{m}_{H2}$) and the net thermal power generated by the oxyfuel boiler ($\dot{Q}_b$) (Equation 2).

$$\xi_{oxy} = \frac{LHV_{H2} \cdot \dot{m}_{H2}}{\dot{Q}_b} \left[\frac{kW_{H2}}{kW_{th}}\right] \quad \text{(Eq. 2)}$$

Coal was selected as input material since it represents the most extended fossil fuel for thermal energy supply in industry [14]. However, in order to achieve an entirely renewable system, it has been replaced by biomass (Table 1). The substitution of the fuel in the oxycombustion boiler directly influences on the operation ranges since carbon, oxygen and water contents in the fuel composition differ significantly. Furthermore, the use of biomass implies other technical

risks that should be considered in the design of the installation such as structural changes in flames that impose shorter particle sizes in biomass oxycombustion [15] or higher H_2O concentrations inside the combustion chamber [16]. However, the study of these issues are beyond the scope of this paper.

Table 1. Ultimate analysis of selected energy crop [w.b.] [17].

C	H	O	N	S	M	Z
43.9	5.5	41.6	0.3	0.0	5.5	3.2
	Volatile Matter		Fixed Carbon		LHV [MJ/kg]	
	74.0		17.3		17.8	

The entire hybrid system has been modelled in Aspen Plus® by combining and interconnecting an oxyfuel boiler, a CO_2 storing-compression train, an electrolyser and a methanation plant. The oxyfuel boiler is assumed to operate with 15 % of oxygen excess provided by three available sources of O_2, namely, ASU, electrolyser and recirculated flue gas.

The CO_2 train consists of three compressors with pressure ratios of 3.5 and a fourth one with pressure ratio of 3.0, achieving a final pressure of 91.9 bar. To improve the efficiency of compressors, four intercoolers are installed between compression stages for recovering some thermal energy which might be integrated. The temperature of the gas flow is reduced down to 40 ºC in every stage, thus removing water too and providing a final high purity CO_2 stream (95.6%-vol).

The electrolyser was modelled by programming a user-defined subroutine in Aspen Plus®. Based on literature, water conversion is above 99.9% with an electrical consumption range from 4.3 to 4.9 kWh/Nm^3H_2 and an operation temperature around 80 °C [18][19]. The influence of the electrolyser efficiency in the overall performance of the hybrid plant was already studied in

a previous work [13]. In this case, the consumption is set on 4.4 kWh/Nm^{3}H$_2$ ($\eta_{ele,LHV}$ = 61.8 %) since it does not have any influence in the scope of the present study, the available heat by-produced during the process.

Finally, methanation plant is designed to achieve a methane molar fraction above 95 % in the final SNG, which corresponds with the threshold concentration in Spanish legislation for injection in the Natural Gas grid [20]. The proposed scheme, shown in Figure 2, is similar to the original TREMP™ process of Haldor Topsøe [21]. It manages three adiabatic reactors at 30 bar with an intermediate condensation stage and a recirculation over the first methanator.

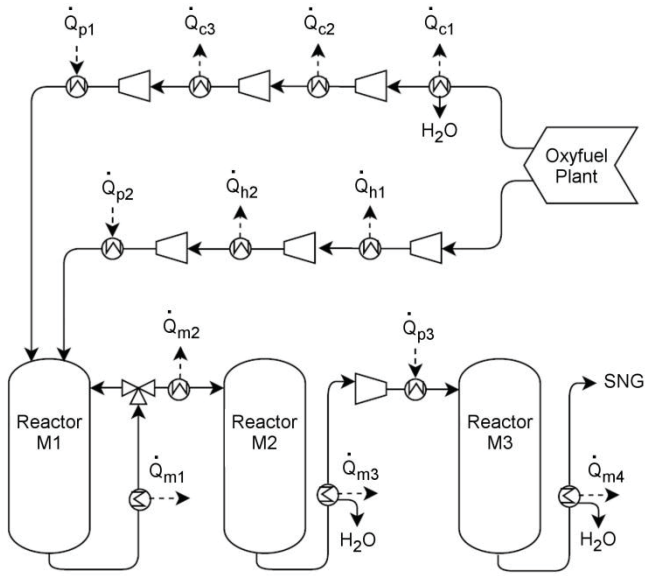

Figure 2. Methanation plant model in Aspen Plus®.

To calculate the percentage of flue gas directed to methanation, ϕ_{FGM}, two system conditions must be taken into account. Firstly, a constant H_2:CO_2 molar ratio of 4 is set at the inlet of the reactor M1 according to the stoichiometry of Equation 1. Then, the presence of oxygen entering the methanator should be avoided since it would poison the catalysts [22]. Thus, it is consumed by a controlled combustion with a small amount of the hydrogen from electrolysis. These two conditions are used to derive Equation 3. The last parameter, $\dot{n}_{CO_2,Loss}$, refers to the CO_2 lost

with water in the condensation stage prior the first reactor. Water is removed from the system since a large presence of steam inhibits methanation reaction.

$$\phi_{FGM} = 100\left[\left(y_{CO_2,FG} + \frac{1}{2}y_{O_2,FG}\right)^{-1}\frac{(\dot{n}_{H_2}/4+\dot{n}_{CO_2,Loss})}{\dot{n}_{FG}}\right] \quad \text{(Eq. 3)}$$

Hydrogen and flue gas are passed through compression trains (30 bar) with intermediate cooling stages down to 120 ºC for heat recovering. A preheating stage up to 300 ºC is also required before the first methanator [23]. Then, the composition and temperature of outlet gas are calculated at equilibrium state, minimizing Gibbs free energy in an adiabatic process.

Due to the loss of active surface area in the catalyst above 600 ºC [24], the 80 % of M1's outlet have to be cooled (300 ºC) and recirculated to maintain the process temperature around 550 °C. Thus, the exothermic energy of the Sabatier reaction can be easily recovered as high pressure steam [25]. This thermal energy and the one from the intercooling stages of compression trains, could be integrated at different temperatures (Table 2) improving the overall efficiency.

Then, temperature of the remaining stream is reduced to 250 ºC before entering M2. Lower inlet temperatures are typical in second and following methanators of commercial SNG processes like TREMP® since they promote the upgrading of syngas [26]. Later, the steam content in the outlet gas is partially condensed to avoid the inhibition of methanation reaction. However, an excessively low steam molar fraction could generate solid carbon depositions [2]. In the studied scheme, the third reactor will not produce solid carbon when the temperature of the intermediate condensation stage remains above 125.5 ºC, so temperature at this point is considered to be 130.0 ºC.

The third reactor, M3, also operates without recirculation since high pressure favours methane formation. Its inlet stream is preheated to 250 ºC and the outlet gas is cooled down to 40 °C to condense steam and reach a purity of methane over 95%.

3. Available thermal energy flows

The different subsystems in the hybrid plant present different cooling needs, from which thermal energy can be recovered for integration purposes. Part of this cooling requirements comes from the storage train in its condensation stages ($\dot{Q}_{s1}$, $\dot{Q}_{s2}$, $\dot{Q}_{s3}$ and $\dot{Q}_{s4}$). Similarly, thermal energy must be extracted from the intercoolers of the hydrogen ($\dot{Q}_{h1}$ and $\dot{Q}_{h2}$) and flue gas ($\dot{Q}_{c1}$, $\dot{Q}_{c2}$ and $\dot{Q}_{c3}$) compression trains. Lastly, in the methanation plant four more energy streams are removed to mitigate the heat released by exothermic Sabatier reaction ($\dot{Q}_{m1}$, $\dot{Q}_{m2}$, $\dot{Q}_{m3}$ and $\dot{Q}_{m4}$).

The available specific energy of each stream, defined as the total amount of thermal energy that must be removed to fulfil cooling requirements (Eq. (4)), is shown in Table 2.

$$\dot{Q}_{j,i} = \dot{m}_{j,i} \cdot cp_{j,i} \cdot \Delta T_{j,i} \qquad j = s,h,c,m\,; \quad i = 1,2,... \qquad \text{(Eq. 4)}$$

Depending on the source, heats are normalized with respect to different variables avoiding the influence of ξ_{oxy}. Compression heats are normalized with respect to the inlet mass flows, whilst methanation heat has been divided by the amount of hydrogen produced in the electrolyser. Thus, data of available thermal energy for external integration are valid for every ξ_{oxy}. It should be noted that values of available energy are not comparable for different sub-systems due to the distinct normalization.

Table 2. Available specific energies from CO_2 compression [$kW_t/(t_{CO2}/h)$], hydrogen compression [$kW_t/(t_{H2}/h)$], flue gas compression [$kW_t/(t_{CO2}/h)$] and methanation [$kW_t/(t_{H2}/h)$].

	Stream temperature [ºC]	Final temperature [ºC]	Available specific energy	Waste energy in condensed water*
$\dot{Q}_{s1}$	330.8	40.0	159.2	1.7
$\dot{Q}_{s2}$	144.7	40.0	33.2	0.2
$\dot{Q}_{s3}$	144.4	40.0	28.8	0.2
$\dot{Q}_{s4}$	130.6	40.0	23.7	-

$\dot{Q}_{h1}$	223.9	120.0	419.4	-
$\dot{Q}_{h2}$	279.9	120.0	645.9	-
$\dot{Q}_{c1}$	190.0	40.0	90.9	1.1
$\dot{Q}_{c2}$	131.7	120.0	3.4	-
$\dot{Q}_{c3}$	226.5	120.0	32.0	-
$\dot{Q}_{m1}$	539.7	300.0	5826.8	-
$\dot{Q}_{m2}$	300.0	250.0	224.7	-
$\dot{Q}_{m3}$	380.4	130.0	3485.8	498.8
$\dot{Q}_{m4}$	328.7	40.0	1052.4	12.6

* Energy content of condensed water in the cooling stage, reference 25 ºC.

As shown in Table 2, there exist several lower limits for the final temperatures due to technical aspects. In the compression train for CO_2 storage and the condensation stage prior the flue gas compression to methanation, the temperature of condensers is set as 40 ºC and the cooling process can be carried out with water at ambient temperature. However, the intercooling phases of hydrogen and flue gas compression are limited to 120 ºC since a subsequent preheating up to 300 ºC is required. In the methanation plant, $\dot{Q}_{m1}$ and $\dot{Q}_{m2}$ streams cannot be cooled below 300 ºC and 250 ºC respectively, since they are introduced in the reactors and a minimum operating temperature must be ensured. In addition, the heat removed in $\dot{Q}_{m3}$ is limited since an excessive steam condensation in this point will produce solid carbon deposition in the third methanator. Therefore the minimum acceptable temperature for this intermediate condensation is 130 ºC. Finally, $\dot{Q}_{m4}$ belongs to a steam condensation stage, which is performed at 40 ºC.

Despite all this available energy, only a fraction will be exchanged between hot streams and internal ($\dot{Q}_{p1}$, $\dot{Q}_{p2}$ and $\dot{Q}_{p3}$) or external cold streams due to these temperature limitations. In this study, the maximum energy recovery from integration will be defined as useful thermal energy. Furthermore, the waste energy contained in the condensed water that is extracted from the facility is calculated in reference to 25 ºC and also included in Table 2.

4. Efficiency definition and potential improvement

The efficiency of the system will be highly influenced by the operational variations that the hybrid plant suffers through the increment of the ratio ξ_{oxy}. The key operation points for the hybrid system depend on the fuel composition; they are calculated and shown in Figure 3 for an oxyfuel boiler fed with biomass whose composition has been presented in Table 1.

Depending on the value of the ratio between boiler and electrolyser size, ξ_{oxy}, different strategies of operation may be followed in the PtG-oxycombustion hybridized plant: (i) for a given value, ξ_{ASU}, enough oxygen is produced in the electrolyzers to completely fed the oxyfuel boiler and therefore ASU becomes unnecessary; and (ii) for ξ_{CO2}, the flue gas flow produced in the oxyfuel combustion is completely reused and converted to SNG.

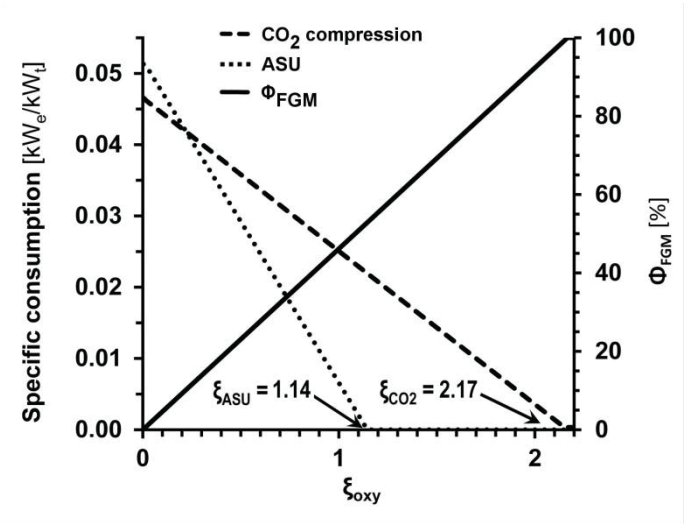

Figure 3. Specific consumptions and percentage of methanised flue gas vs ξ_{oxy}

The results from a previous study of the hybrid PtG-oxycombustion system fired by coal showed the following size ratios for ASU elimination and total CO_2 consumption: $\xi_{ASU} = 1.33$ and $\xi_{CO2} = 2.29$ [13]. The use of biomass in the boiler allows for reducing the size ratio requirement which avoids the need of ASU since oxygen content in biomass is much greater than in coal. In addition, given the smaller C:H ratio in biomass which limits the amount of carbon dioxide generated in the boiler per kW_{th}, the value of ξ_{oxy} to convert entirely the flue

gas is reduced. Nevertheless, those variation in characteristic size ratios as a function of fuel type is beyond the scope of this paper and it is proposed as a further study.

The maximum efficiency of the hybrid system, once the additional available energy streams are considered, can be written down as equation 5.

$$\eta_{PtG+oxy} = \frac{\dot{Q}_b + LHV_{SNG}\dot{m}_{SNG} + \sum_{i=1}^{4}\dot{Q}_{s,i} + \sum_{i=1}^{2}\dot{Q}_{h,i} + \sum_{i=1}^{3}\dot{Q}_{c,i} + \sum_{i=1}^{4}\dot{Q}_{m,i}}{LHV_f\dot{m}_f + \dot{W}_{aux,oxy} + \dot{W}_{ASU} + \dot{W}_{Comp} + \dot{W}_{ele} + \dot{W}_{aux,meth}} \quad \text{(Eq. 5)}$$

The global efficiency of the system accounts for the chemical energy contained in the synthetic methane and the available heat from the boiler and other sources. In this first approach, the entire available thermal energy from compression trains and methanation are considered useful heat. Figure 4 illustrates the comparison between the global efficiency of a non-integrated system and a system where complete use of the available heat is accomplished (Table 2). The rest of possibilities, i.e. the partial use of the available heat due to exchanger temperature limitations, will be intermediate curves. In addition, it should be noted that the electrolyser consumption appears in Equation 5, so the final value of the overall efficiency is actually influenced by the electrolyser performance. However, this effect was neglected since the gap between both limit situations behaves similarly in the possible range of electrolyser efficiency.

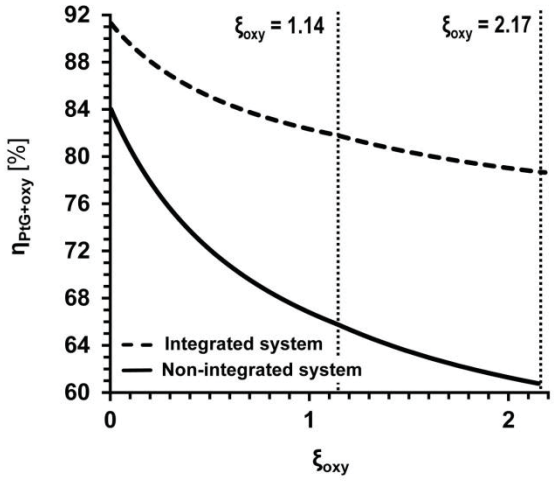

Figure 4. Hybrid plant efficiency vs ξ_{oxy} (w and w/o energy integration)

It is worthy to note that the system without Power to Gas ($\xi_{oxy} = 0$) still observes an improvement in the global efficiency since the heat from the compression train could be potentially integrated. As the share of PtG increases in the hybrid plant, overall efficiency decreases since Power to Gas presents a more limited performance than the oxyfuel boiler. However, the fall in efficiency is partially buffered thanks to the utilization of the waste energy from different sources, mainly methanation heat.

The available heat from compression trains and methanation are grouped by source (Equation 6) and presented in Figure 5 for illustrating their behaviour against ξ_{oxy}. Furthermore, all of them have been normalized regarding the net thermal output of the boiler for direct comparison. It must be highlighted the difference in order of magnitude between the methanation heat and the other sub-systems.

$$Q_j = \sum_i Q_{j,i} \qquad j = s, h, c, m \qquad \text{(Eq. 6)}$$

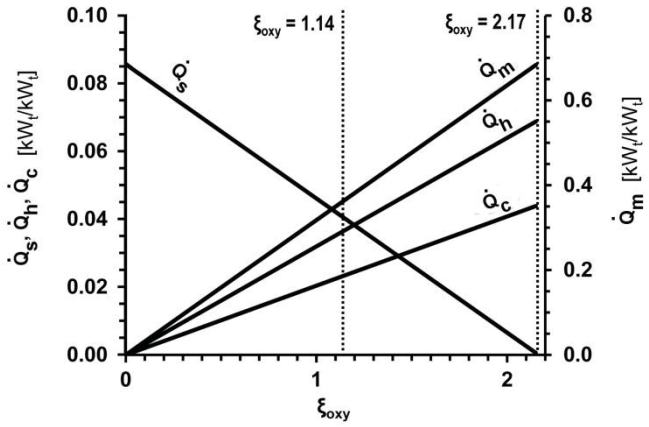

Figure 5. Available specific heats vs ξ_{oxy}

Data from Table 2 show how the ratio between $Q_{j,i}$ for a given j is conserved with ξ_{oxy}. Thus, it can be seen that the 55 % of the methanation heat is always released in $\dot{Q}_{m1}$ (Figure 6).

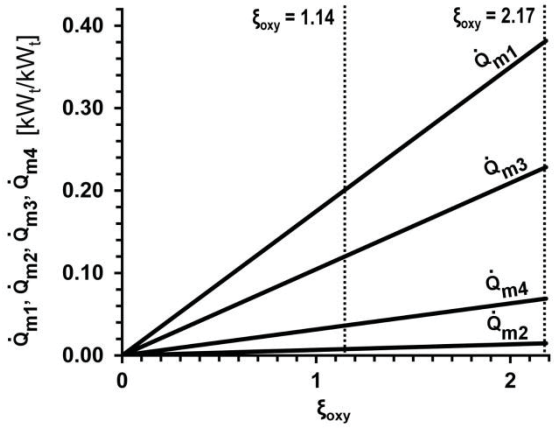

Figure 6. Available specific heats from methanators vs ξ_{oxy}

5. Potential applications

The final application of the PtG-oxy plant will define the adequate operation point, the required equipment and its suitability. Five generic scales for the concept, based on literature, are analysed to determine its technical and economic feasibility: households, district heating (DH), industry, biomass power plants and co-firing (Table 3).

Table 3. Generic applications and characteristics for PtG-biomass oxycombustion at different scales.

Application	Boiler [MW]	ξ_{oxy}	Electrolyser [MW]	SNG [MW]	Technical feasibility	Economic feasibility
Households	0.01	ξ_{ASU} - 1.15·ξ_{ASU}	0.02	0.01	✓	-
District heating	2	ξ_{ASU} - 1.15·ξ_{ASU}	3.4 - 3.9	1.7 - 2.0	✓	✓
Industry	20	ξ_{ASU} - ξ_{CO2}	33.5 - 63.7	16.8 - 31.9	✓	✓
Power plant	200	ξ_{ASU} - ξ_{CO2}	335 - 637	168 - 319	-	✓
Co-firing	1000	0.8·ξ_{CO2} - ξ_{CO2}	2549 - 3186	1275 - 1593	-	✓

Note: Electrolyser efficiency 68.1% (LHV)

Typical household heating consumption in a cold climate region is laid in the range 60 – 200 kWh/m^2/yr [27]. Therefore, assuming 1500 hours of operation per year [28], a 150 kWh/m^2/yr moderate specific consumption and a 90 m^2 household, the required boiler power is around 10 kW_{th}.

District heating size distribution varies remarkably from one country to another. In Finland and Denmark, which are northern Europe countries, majority of the DH systems are larger than 10 MW_{th} and rarely smaller than 2 MW_{th}. Moreover, there exist a relevant number of DH facilities with powers higher than 100 MW_{th}. However, in Switzerland (central Europe) the district heating systems are predominantly in the range 1 - 5 MW_{th} with an important amount of plants even smaller than 1 MW_{th} [29]. Consequently, the percentage of citizens that have access to district heating networks in the two first cases is 50 % and 60 % respectively, whilst in Switzerland this share drops below 5 % [30]. Nevertheless, heat-only boilers for district heating are normally used as backup when peak demands are uncovered [31], so small sizes are more suitable for this scope. Thus, a 2 MW_{th} boiler size would be a representative size for a PtG-biomass oxycombustion hybrid plant used in district heating.

Industry boiler applications and their average capacities can be summarized in five main fields: chemicals (10.0 MW_{th}), paper (31.4 MW_{th}), food (5.9 MW_{th}), refining (33.2 MW_{th}) and metals (9.2 MW_{th}), where typical sizes for each sector have been estimated from United States data [32]. Thus, the average value for an industrial boiler for these five sectors would be around 18 MW_{th}.

Direct combustion biomass plants are commercially available from a few MW_e to 300 MW_e, and are the most common form of power generation with this renewable fuel (90 % of the biomass used for energy purposes is combusted) [33]. Plants which are compatible with the availability of local biomass feedstock are usually limited to 50 MW_e, whilst those that are supplied by internationally traded biomass may reach 300 MW_e [34]. A 50 MW_e power plant is taken here as a generic case. Efficiency of biomass power plants in the 50 MW_e size range are between 18 % and 33 % [34], so 26 % efficiency is selected as a representative case. Hence, the boiler power that this power plant would need is around 192 MW_{th}.

In the co-firing case, the largest plant has a 4000 MW_e capacity (North Yorkshire, property of Drax Power, 6x660 MW_e), whilst the following nine larger facilities have a total capacity in the

range 1960 – 2400 MW_e [35]. However, currently the typical direct co-firing plant sizes are between 10 – 1000 MW_e, with a net electric efficiency between 35 – 42 % [36]. Thus, the chosen generic case is a 500 MW_e plant with an intermediate efficiency value (38.5 %), which would need a 1.3 GW_{th} boiler.

The selection of operation point must be in accordance to the scale of the plant and its final purpose. Hence, small scale installations (households and DH) are not compelled to capture their emissions since the amount of produced CO_2 will not be large enough. Thus, an operation point around ξ_{ASU} would be recommended. In medium and large scale facilities, such as industrial applications or power plants, to avoid greenhouse gas emissions might be mandatory and economically interesting. However, these applications could be operated in a wider range between ξ_{ASU} and ξ_{CO2} without restrictions given the neutrality in CO_2 emissions of biomass combustion. Contrary, co-firing facilities cannot take advantage of biomass neutral emissions, and they will be compelled to capture their carbon dioxide. Therefore, a range next to ξ_{CO2} would be the most suitable operation for those applications (Figure 7).

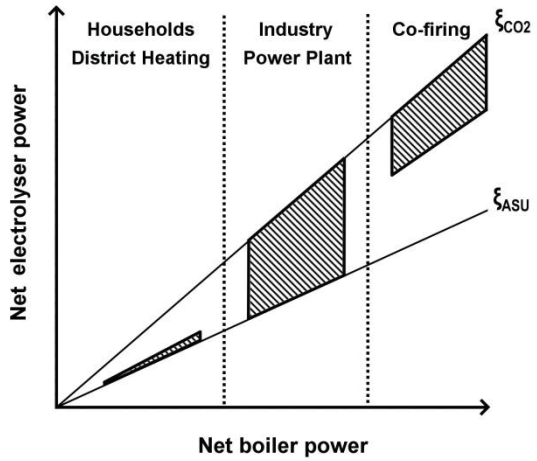

Figure 7. Map of operation points for different scale facilities

Once the adequate range of electrolyser size is fixed for each scale, the technical feasibility is determined by the state of the art of the electrolysis technology. Nowadays, electrolysers are

commercially available from a few kW_e up to 2 MW_e [37]. Therefore, it may be considered that there is no lower limit but an upper one, which implies that industrial uses are the largest possible applications through the combination of fifteen to thirty units of 2 MW_e size electrolysers. Hence, the next scale steps (power plants and co-firing), would require more than 160 of these electrolysers, so it is assumed that there is not any technical feasibility in these cases.

Finally, the economic feasibility is assessed as a function of the SNG production capacity taken from the results presented in the final report of the *TKI power-to-gas system analysis project* developed in Rozenburg (Figure 8) [38].

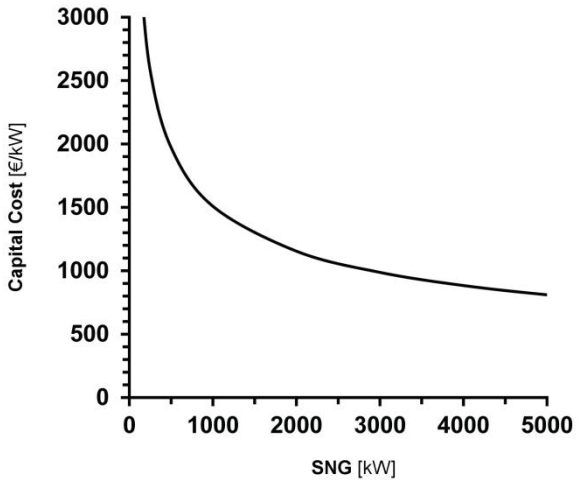

Figure 8. Capital cost for methanation plants [38]

The amount of SNG generated under each potential application is calculated using the efficiency obtained through Aspen Plus simulations ($\eta_{PtG} \cong 50\ \%$). From these calculations it is obtained that the application in households of the PtG-oxy hybrid system would present unbearable capital and operational costs while for larger scales these costs are strongly attenuated.

In conclusion, under current conditions only district heating and industry applications seem to be technically and economically feasible for a PtG-biomass oxycombustion hybrid plant.

Therefore, these both cases are briefly analysed in the two following sections. However, with a mature PtG technology and a greater electrolyser development, smaller and larger applications could be also suitable.

5.1. District heating

Heating and domestic hot water (DHW) necessities in residential buildings account for 75% of their total energy consumption [39]. A study performed by Carpio et al. [40] shows that the replacement of diesel with biomass, in Spanish residential building heating, leads to CO_2 emission reductions between 82.9 % and 95.3 %, whilst whether natural gas is replaced, emissions would drop between 77.4 % and 93.7 %. The proposal of a PtG-biomass oxyfuel boiler for district heating is, thus, well justified.

In 2014, the concept of 4th Generation District Heating (4GDH) was defined. Its main advantage is the increment in efficiency due to the lower distribution temperatures (30 - 70 ºC) [41]. Several 4GDH projects funded by the IEA-DHC research programme have been finalized and other new four projects will be executed during the 2014-2017 period [42]. However, given the fact that the 4GDH approach is still under research, the technical parameters accounted in this study are based on previous district heating generations.

The 3rd Generation DH systems usually are operated at end costumer supply temperatures between 80 - 100 ºC [43], and pressures above 6 bar [44]. However, hot water transportation from DH plants to end user distribution network is made by transmission networks whose design parameters are more robust. The rigid plastic jacket pipes are the most widely used (140 ºC and 25 bar) because of their greater standardization and lower prices [29], so these characteristics are chosen for the present case study.

The waste heat from PtG-biomass oxycombustion plant is recovered in a series of exchangers with a minimum difference of 20 ºC between cold and hot streams. Therefore, the lower limit temperature to cool down the hot streams is 160 ºC. Under this situation, $\dot{Q}_{m1}$ and $\dot{Q}_{m2}$ will be

exhausted, $\dot{Q}_{s2}$, $\dot{Q}_{s3}$, $\dot{Q}_{s4}$ and $\dot{Q}_{c2}$ cannot be used, and the remaining heats will be only partially recovered. The useful energy that can be extracted from each point and the amount of water heated to 140 ºC and 25 bar are shown in Table 4.

Table 4. Percentage of available specific heat (Table 2) that is useful in DH systems, and data for the generic case (2 MW_{th} at ξ_{ASU}, Table 3).

	Useful specific heat [%]	Useful heat [kW]	Produced hot-water [kg/h]
$\dot{Q}_{s1}$	37.5	19.7	118.0
$\dot{Q}_{s2}$	0.0	0.0	0.0
$\dot{Q}_{s3}$	0.0	0.0	0.0
$\dot{Q}_{s4}$	0.0	0.0	0.0
$\dot{Q}_{h1}$	61.5	17.7	106.1
$\dot{Q}_{h2}$	75.0	33.3	199.5
$\dot{Q}_{c1}$	11.1	3.7	22.2
$\dot{Q}_{c2}$	0.0	0.0	0.0
$\dot{Q}_{c3}$	63.3	7.5	44.9
$\dot{Q}_{m1}$	100.0	399.9	2396.3
$\dot{Q}_{m2}$	100.0	15.4	92.3
$\dot{Q}_{m3}$	93.9	224.5	1345.2
$\dot{Q}_{m4}$	43.3	31.3	187.6
Total	81.2	753.0	4512.1

Given the limited amount of GHG emissions in district heating systems, to install a capture and compression facility for the CO_2 is not mandatory. Therefore, the heat recovered from the compression train may compute or not when calculating the efficiency of the system. In Figure 9 the efficiencies under both scenarios together with the lower and upper limits of the base case (Figure 4) are represented.

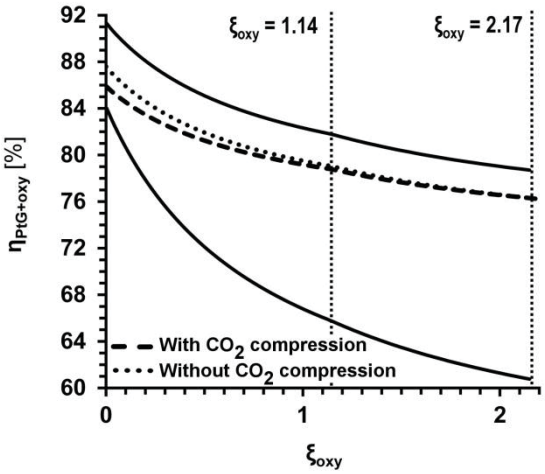

Figure 9. Hybrid plant efficiency vs ξ_{oxy} (DH application)

Initially, the inclusion of a CO_2 compression stage in the integrated system implies a reduction in the efficiency. However, once the ASU becomes unnecessary this penalty disappears and both systems have barely the same efficiency, because the greater influence of the PtG process against the compression heat.

5.2. Industry

Contrary to district heating application where the target of the produced heat is clear and its technical requirements are fixed, industry applications might be oriented to different final uses in a large range of temperatures. Therefore, a general analysis of industry applications similar to the DH analysis cannot be performed. Nevertheless, some aspects of these potential applications can be highlighted.

Pulp and paper manufacturers, as well as chemical industry, are two of the main medium temperature steam consumers that could take advantage of PtG-oxyfuel systems, since chemical industry employ 47 % of their entire energy expenditure for producing steam and paper industry up to 84 % [45]. Furthermore, paper manufacturing generates bark and sawdust as by-product that is commonly used as biofuel for producing steam that is self-consumed [46]. Hence, paper mills are one of the best candidates for a big scale PtG-biomass oxycombustion development.

As a summary, some of the main potential uses included in the paper industry and chemical sector, are shown in Table 5, with their corresponding requirements of temperature and pressure.

Table 5. Requirements for some of the potential uses of steam in paper and chemical industries [45][47][48].

	T_{Steam} [ºC]	P_{Steam} [bar]
Paper industry		
Digesting	170.0	7.9
Chemical recovery	144.4	3.1
Bleaching	126.7	1.4
Drying	126.7	1.4
Chemical industry*		
Distillation	121.1	1.0
Drying	187.8	11.0
Blending	121.1	1.0
Melt compounding	146.1	3.5

*PVC production case

The strong differences between steam requirements in a specific process together with the availability of multiple thermal energy flows coming from the PtG-Oxycombustion boiler, suggest the utilization of the pinch analysis technique for maximizing the overall net efficiency. There exists huge potential for integration between industry and the proposed hybrid technique and the possibility of greater development through further specific studies.

6. Conclusions

A PtG-Oxycombustion hybrid system which transforms electricity from renewable sources and heat from biomass combustion into carbon-neutral synthetic natural gas has been proposed and analysed. In the light of results, the most adequate applications in which this system could be integrated have also been assessed.

Small scale plants are urged to operate near above ξ_{ASU} since lower CO_2 emissions are normally not compelled to be captured through economic penalties, while for large scale facilities is recommended to operate with size ratios next to ξ_{CO2} to ensure the complete conversion of flue gas flow into SNG. Hence, when technical and economic feasibilities of generic cases are evaluated taking into account these assumptions (Table 3), the most suitable applications for the PtG-Oxycombustion hybrid system are found.

The required size for the electrolyser size in the cases of power plants and co-firing applications would be too large to be technically feasible, whilst the thermal energy consumption of household are so small that specific cost of the required plant matching the demand would be extremely high. However, district heating and industrial applications requirements lie in an affordable range for the hybrid system.

In addition, extra thermal energy production from methanation and compression trains is quantified to assess the potential increment of global efficiency for these applications. At the operational point ξ_{ASU}, heat integration allows to increase overall net efficiency from 65.7 % to 81.8 %, whilst for ξ_{CO2} from 60.7 % to 78.7 %.

The analysis of a district heating case shows that a 81.2 % of the available heat becomes useful for integration at the recommended operational point ξ_{ASU}, so overall net efficiency is increased up to 78.7 %. If temperature requirements were lower, as in 4GDH systems, useful heat and efficiency would be even greater.

Further studies are proposed in order to analyse the influence of the type of fuel used in the boiler. First results indicates that oxygen content and C:H ratio produce remarkable modifications in the values of ξ_{ASU} and ξ_{CO2}, respectively.

Lastly, the boundaries of the system should be extended in order to perform a ‘full-fuel-cycle’ analysis of the proposed concepts and to estimate the emission factors and losses associated

412 with the power generation. This analysis would allow a realistic assessment of the concept
413 under a specific scenario in comparison to other available energy storage technologies.

414 **Acknowledgements**

415 The authors would like to acknowledge funding from Fundación Iberdrola through the program
416 "Ayudas a la Investigación en Energía y Medioambiente" 2014 – 2015.

417 **Abbreviations**

4GDH	4th generation district heating
ASU	Air separation unit
DH	District heating
DHW	Domestic hot-water
LHV	Lower heating value
M	Moisture
M1	Methanator 1
M2	Methanator 2
M3	Methanator 3
PtG	Power to Gas
SNG	Synthetic natural gas
Z	Ash

418

419 **Nomenclature**

Variables

cp	Specific heat at constant pressure [kJ/kg·K]
LHV	Lower heating value [kJ/kg]
$\dot{m}$	Mass flow [kg/s]
$\dot{n}$	Molar flow [kmol/s]
P	Pressure [bar]
$\dot{Q}$	Thermal power [kWt]
T	Temperature [K]
$\dot{W}$	Electric power [kWe]
y	Molar fraction [-]
η	Efficiency [%]
ξ_{ASU}	Minimum required ratio between electrolyser power and boiler net output to avoid ASU necessity [kWe/kWt]
ξ_{CO2}	Minimum required ratio between electrolyser power and boiler net output to consume flue gas completely [kWe/kWt]
ξ_{oxy}	Ratio between electrolyser power and boiler net output [kWe/kWt]
ϕ_{FGM}	Percentage of flue gas directed to methanation [%]

Subscripts

ASU	Air separation unit
aux	Auxiliary consumption

b	Boiler
CO_2	Carbon dioxide
$comp$	CO_2 compression
e	Electric
ele	Electrolyser
f	Fuel
FG	Flue gas
H_2	Hydrogen
$Loss$	Losses in condensation phase prior M3
M	Methanator
$meth$	Methanation
O_2	Oxygen
oxy	Oxyfuel plant
PtG	Power to Gas
$PtG + oxy$	Power to Gas-Oxyfuel hybrid system
SNG	Synthetic natural gas
th	Thermal

References

[1] Vandewalle J, Bruninx K, D'haeseleer W. Effects of large-scale power to gas conversion on the power, gas and carbon sectors and their interactions. Energy Convers Manag 2015;94:28–39. doi:10.1016/j.enconman.2015.01.038.

[2] Gao J, Wang Y, Ping Y, Hu D, Xu G, Gu F, et al. A thermodynamic analysis of methanation reactions of carbon oxides for the production of synthetic natural gas. RSC Adv 2012;2:2358. doi:10.1039/c2ra00632d.

[3] Schneider L, Kötter E. The geographic potential of Power-to-Gas in a German model region - Trier-Amprion 5. J Energy Storage 2015;1:1–6. doi:10.1016/j.est.2015.03.001.

[4] Sterner M. Bioenergy and renewable power methane in integrated 100% renewable energy systems (Thesis). Kassel University Press GmbH, 2009. ISBN 978-3-89958-798-2.

[5] Thrän D, Billing E, Persson T, Svensson M, Daniel-Gromke J, Ponitka J, et al. Biomethane, Status and Factors Affecting Market Development and Trade. IEA Bioenergy, 2014. ISBN 978-1-910154-10-6.

[6] Iskov H, Rasmussen N. Global screening of projects and technologies for Power-to-Gas and Bio-SNG. Project Report. Danish Gas Technology Centre, 2013. ISBN 978-87-7795-373-6.

[7] Kirchmayr M. Power-to-Gas: Modellierung der Energieverwertungspfade und Einflussnahme einer veränderten Strommarktsituation. Diplomica Verlag GmbH; 2014. ISBN 3842893914.

[8] Denmark turns excess wind power into gas via Hydrogenics tech. Fuel Cells Bull 2014;2014:8–9. doi:10.1016/S1464-2859(14)70082-3.

[9] Szwaja S, Kovacs VB, Bereczky A, Penninger A. Sewage sludge producer gas enriched with methane as a fuel to a spark ignited engine. Fuel Process Technol 2013;110:160–6. doi:10.1016/j.fuproc.2012.12.008.

[10] Persson T, Murphy J, Jannasch A-K, Ahern E, Liebetrau J, Trommler M, et al. A perspective on the potential role of biogas in smart energy grids. IEA Bioenergy, 2014. ISBN 978-1-910154-12-0.

[11] Wall T, Liu Y, Spero C, Elliott L, Khare S, Rathnam R, et al. An overview on oxyfuel coal combustion-State of the art research and technology development. Chem Eng Res Des 2009;87:1003–16. doi:10.1016/j.cherd.2009.02.005.

[12] Hu Y, Li X, Li H, Yan J. Peak and off-peak operations of the air separation unit in oxy-coal combustion power generation systems. Appl Energy 2013;112:747–54. doi:10.1016/j.apenergy.2012.12.001.

[13] Bailera M, Lisbona P, Romeo LM. Power to gas-oxyfuel boiler hybrid systems. Int J Hydrogen Energy 2015. doi:10.1016/j.ijhydene.2015.06.074.

[14] Eisentraut A, Brown A. Heating without global warming - Market developments and policy considerations for renewable heat. International Energy Agency, Paris, 2014.

[15] Holtmeyer ML, Kumfer BM, Axelbaum RL. Effects of biomass particle size during cofiring under air-fired and oxyfuel conditions. Appl Energy 2012;93:606–13. doi:10.1016/j.apenergy.2011.11.042.

[16] Jurado N, Darabkhani HG, Anthony EJ, Oakey JE. Oxy-combustion Studies Into the Co –Firing of Coal and Biomass Blends: Effects on Heat Transfer, Gas and Ash Compositions. Energy Procedia 2014;63:440–52. doi:10.1016/j.egypro.2014.11.047.

[17] Pickard SC, Daood SS, Pourkashanian M, Nimmo W. Co-firing coal with biomass in oxygen- and carbon dioxide-enriched atmospheres for CCS applications. Fuel 2014;137:185–92. doi:10.1016/j.fuel.2014.07.078.

[18] Tijani AS, Yusup NAB, Rahim a. HA. Mathematical Modelling and Simulation Analysis of Advanced Alkaline Electrolyzer System for Hydrogen Production. Procedia Technol 2014;15:799–807. doi:10.1016/j.protcy.2014.09.053.

[19] Dieguez P, Ursua a, Sanchis P, Sopena C, Guelbenzu E, Gandia L. Thermal performance of a commercial alkaline water electrolyzer: Experimental study and mathematical modeling. Int J Hydrogen Energy 2008;33:7338–54. doi:10.1016/j.ijhydene.2008.09.051.

[20] BOE-A-2013-185. Resolución de 21 de diciembre de 2012, de la Dirección General de Política Energética y Minas, por la que se modifica el protocolo de detalle PD-01. Ministerio de Industria, Energía y Turismo; 2013.

[21] Kopyscinski J, Schildhauer TJ, Biollaz SM a. Production of synthetic natural gas (SNG) from coal and dry biomass - A technology review from 1950 to 2009. Fuel 2010;89:1763–83. doi:10.1016/j.fuel.2010.01.027.

[22] Agersborg J, Lingehed E. Integration of Power-to-Gas in Gasendal and GoBiGas. Master's Thesis Report No. T2013-396. Chalmers University of Technology, 2013.

[23] Nguyen TTM, Wissing L, Skjøth-Rasmussen MS. High temperature methanation: Catalyst considerations. Catal Today 2013;215:233–8. doi:10.1016/j.cattod.2013.03.035.

[24] Rostrup-Nielsen JR, Pedersen K, Sehested J. High temperature methanation. Sintering and structure sensitivity. Appl Catal A Gen 2007;330:134–8. doi:10.1016/j.apcata.2007.07.015.

[25] Sudiro M, Bertucco a. Synthetic Natural Gas (SNG) from coal and biomass: a survey of existing process technologies, open issues and perspectives. Nat Gas 2010:105–27. doi:10.5772/9835.

[26] Heyne S, Seemann MC, Harvey S. Integration study for alternative methanation technologies for the production of synthetic natural gas from gasified biomass. Chem Eng Trans 2010;21:409–14. doi:10.3303/CET1021069.

[27] Edenhofer O, Pichs-Madruga R, Sokona Y, Farahani E, Kadner S, Seyboth K, Adler A, Baum I, Brunner S, Eickemeier P, Kriemann B, Savolainen J, Schlömer S, Stechow C, Zwickel T, Minx JC. Climate Change 2014: Mitigation of Climate Change. Contribution of Working Group III to the Fifth Assessment Report of the Intergovernmental Panel on Climate Change. IPCC, 2014. ISBN 978-1-107-05821-7.

[28] IDAE. Guía técnica de instalaciones de biomasa térmica en edificios. Instituto para la Diversificación y Ahorro de la Energía, 2009. ISBN 978-84-96680-46-3.

[29] Nussbaumer T, Thalmann S. Status Report on District Heating Systems in IEA Countries. Swiss Federal Office of Energy, 2014. ISBN 3-908705-28-2.

[30] Colmenar-Santos A, Rosales-Asensio E, Borge-Diez D, Mur-Pérez F. Cogeneration and district heating networks: Measures to remove institutional and financial barriers that restrict their joint use in the EU-28. Energy 2015;85. doi:10.1016/j.energy.2015.03.088.

[31] United Nations Environment Programme. District Energy in Cities - Unlocking the Potential of Energy Efficiency and Renewable Energy. 2015.

[32] Energy Technology Systems Analysis Programme. Industrial Combustion Boilers. Techonology Brief I01-May. International Energy Agency-ETSAP, 2010.

[33] IRENA. Biomass for Power Generation, In: Renewable Energy Technologies: Cost Analysis Series, Vol. 1: Power Sector, Issue 1/5. International Renewable Energy Agency, 2012.

[34] Eisentraut A, Brown A. Technology Roadmap - Bioenergy for Heat and Power. International Energy Agency, IEA Renewable Energy Division, 2012. ISBN 9789264123236.

[35] Vakkilainen E, Kuparinen K, Heinimö J. Large Industrial Users of Energy Biomass - Report for IEA Bioenergy Task 40. Lappeenranta University of Technology, 2013.

[36] Lempp P. Biomass Co- firing. Techonology Brief E21 - January. International Energy Agency-Energy Technology Systems Analysis Programme (IEA-ETSAP), and International Renewable Energy Agency (IRENA), 2013.

[37] Sharma S, Ghoshal SK. Hydrogen the future transportation fuel: From production to applications. Renew Sustain Energy Rev 2015;43:1151–8. doi:10.1016/j.rser.2014.11.093.

[38] Grond L, Schulze P, Holstein J. Systems Analyses Power to Gas - Deliverable 1: Technology Review. Final Report - Project TKIG01038. KEMA Nederland B.V., 2013.

[39] Sharif MKA, Al-abidi a a, Mat S, Sopian K, Ruslan MH. Review of the application of phase change material for heating and domestic hot water systems. Renew Sustain Energy Rev 2015;42:557–68. doi:10.1016/j.rser.2014.09.034.

[40] Carpio M, Zamorano M, Costa M. Impact of using biomass boilers on the energy rating and CO2 emissions of Iberian Peninsula residential buildings. Energy Build 2013;66:732–44. doi:10.1016/j.enbuild.2013.07.079.

[41] Lund H, Werner S, Wiltshire R, Svendsen S, Thorsen JE, Hvelplund F, et al. 4th Generation District Heating (4GDH). Integrating smart thermal grids into future sustainable energy systems. Energy 2014;68:1–11. doi:10.1016/j.energy.2014.02.089.

[42] IEA-DHC. Annex XI 2014-2017. Bringing countries together to research, innovate and grow district heating and cooling - including CHP. International Energy Agency, 2014.

[43] Dalla A, Li H, Svendsen S, Werner S, Persson U, Rehling K. Annex X Final report. Toward 4th Generation District Heating : Experience and Potential of Low-Temperature District Heating. International Energy Agency - DHC, 2014.

[44] Energy Technology Systems Analysis Programme. District Heating. Techonology Brief E16 - January. International Energy Agency-ETSAP, 2013.

[45] U.S. Department of Energy. Steam System Opportunity Assessment for the Pulp and Paper, Chemical Manufacturing, and Petroleum Refining Industries. 2002. doi:DOE/GO-102002-1639.

[46] Isaksson J, Åsblad A, Berntsson T. Influence of dryer type on the performance of a biomass gasification combined cycle co-located with an integrated pulp and paper mill. Biomass and Bioenergy 2013;59:336–47. doi:10.1016/j.biombioe.2013.10.002.

[47] ATECYR. Guía técnica de agua caliente sanitaria central. Instituto para la Diversificación y Ahorro de la Energía, 2010. ISBN 978-84-96680-52-4.

[48] IDAE. Guía práctica sobre instalaciones centralizadas de calefacción y agua caliente sanitaria (ACS) en edificios de viviendas. Información y consejos para las comunidades de vecinos. Instituto para la Diversificación y Ahorro de la Energía, 2008.